Pflügers Arch (1983) 398:48–54

Pflügers Archiv
European Journal of Physiology

Postjunctional characteristics of the endplates in mammalian fast and slow muscles*

Raimund Sterz, Murali Pagala**, and Klaus Peper

II. Pysiologisches Institut, D-6650 Homburg/Saar, Federal Republic of Germany

Abstract. We have studied the postjunctional characteristics of motor endplates in the extensor digitorum longus (EDL) and soleus muscles of the rat. At voltage clamped endplates, equilibrium interactions between acetylcholine (ACh) and the ACh receptor were determined from the dose-response curves obtained by quantitative ionophoresis of ACh. These results showed that the maximum ACh induced conductance change per unit endplate surface, g_{max}, was 21.8 ± 0.9 nS/μm² in EDL and 8.2 ± 0.9 nS/μm² in soleus, the apparent dissociation constant, K, was 65.9 ± 4.3 μM in EDL and 43.5 ± 3.3 μM in soleus, and the Hill-coefficient, n_H, was 2.3 ± 0.1 in EDL and 2.2 ± 0.1 in soleus.

Single channel characteristics were derived from analysis of the ACh-induced endplate current noise. The results showed that at room temperature the mean conductance of the single channel, γ, was 24.6 ± 1.2 pS in EDL and 23.9 ± 1.2 pS in soleus, and the mean life time of the channel, τ, was 0.80 ± 0.05 ms in EDL and 0.71 ± 0.03 ms in soleus.

Of all the properties studied, the maximum conductance per unit endplate surface, g_{max}, was significantly smaller at the soleus endplate than at the EDL endplate. The calculated density of functional ACh receptors was 62% less, and the total number of the functional ACh receptors was 60% less at the soleus endplates than at the EDL endplates. These results suggest that the soleus has a lower margin of safety for neuromuscular transmission than the EDL.

Key words: Neuromuscular junction – Fast and slow muscles – Acetylcholine receptor – Acetylcholine dose-response relations – Noise analysis – Acetylcholine receptor density

Introduction

Mammalian fast and slow muscles differ significantly in their morphology (Stein and Padykula 1962; Ellisman et al. 1976), histochemistry (Nachmias and Padykula 1958; Guth and Samaha 1969; Ariano et al. 1973), biochemistry (Barany et al. 1965; Goldspink et al. 1971; Barnard et al. 1971), electrophysiology (Yonemura 1967; Albuquerque and Thesleff 1968; McArdle and Albuquerque 1973; Tonge 1974) and contractile properties (Close 1964). There are also considerable differences between various characteristics in neuromuscular transmission in these two muscles. Motor endplates of fast muscle fibers receive a higher frequency of motoneuron discharge (Eccles et al. 1958), show a higher frequency of miniature endplate potentials (McArdle and Albuquerque 1973; Tonge 1974), and have a higher quantal content per endplate potential (Tonge 1974) than those of the slow muscle fibers. Postsynaptic sensitivity to acetylcholine (ACh) is restricted to the endplate area in fast muscle fibers, while, though highest at the endplate region, sensitivity can be detected along the entire length of slow muscle fibers (Miledi and Zelena 1966; Albuquerque and McIsaac 1970). However, the maximum "sensitivity" to ACh was reported to be similar at the endplates of both fast and slow muscle fibers (Albuquerque and McIsaac 1970). Since the measurement of ACh sensitivity does not describe the equilibrium interactions between ACh and ACh receptors (Peper et al. 1982), we have determined the ACh dose-response relationship by quantitative ionophoresis (Dreyer et al. 1978) at the endplates of fast and slow muscle fibers. In order to further characterize these endplates, single channel properties were determined by analyzing the ACh-induced current fluctuations (Anderson and Stevens 1973; Dreyer et al. 1976b). Some of these results have already been published in abstract form (Sterz et al. 1982).

Materials and methods

Animals. Female Lewis rats weighing 200–250 g (age: 2–3 months) were obtained from the breeding colony of the Max-Planck-Institut for Immunbiologie (Freiburg, FRG).

Muscle preparation. The rat was anaesthetized with ether and killed by dislocation of the neck. The extensor digitorum longus (EDL) from one leg, and the soleus from the other leg, were dissected in an oxygenated physiological solution. The EDL was pinned down, with the dorsal side up, in a Sylgard-filled Petri dish, containing the physiological fluid, and the following procedure adapted so as to obtain monolayers of muscle fibers on which single endplates could be easily visualized with Nomarski-interference optics. Three of the four posterior tendons of the EDL were dissected out together with the associated fascicles of muscle fibers. The fourth fascicle with its tendon was spread out laterally and fixed with micropins. Posterior to the point of nerve entry, a horizontal incison was made with a pair of iridectomy scissors. When the cut muscle fibers retracted, they were gently removed with the tips of a fine forceps. This procedure was repeated until a

Offprint requests to R. Sterz at the above address
* This work was supported by the Deutsche Forschungsgemeinschaft, SFB 38, project N
** *Present address:* Maimonides Medical Center, 4802 Tenth Avenue, Brooklyn, New York

monolayer of muscle fibers with intact nerve terminals was obtained. Then the preparation was carefully transferred to a glass-bottomed recording chamber, made of magnetic stainless steel. A similar microdissection procedure was used to obtain monolayers of muscle fibers from the whole soleus muscle.

Staining procedure. Endplates in monolayer preparations of EDL and soleus were stained for ACh esterase following the method of Karnovsky and Roots (1964). The surface area of the endplates was evaluated by planimetry of enlarged photographs of endplates which had been stained for ACh esterase. A correction for the curvature of the muscle fibers was not made.

Solutions. The physiological saline solution had the following composition (mM): NaCl 135, KCl 5, $CaCl_2$ 1, $MgCl_2$ 1, Na_2HPO_4 1, $NaHCO_3$ 15 and glucose 11 and was oxygenated and maintained at pH 7.2 by constant bubbling with a gas mixture of 95 % O_2 and 5 % CO_2. It was continously perfused through the recording chamber at 1 ml/min. The experiments were carried out at room temperature (20 – 22° C).

Electrophysiology. Dose-response relationships were determined by performing quantitative ionophoresis as previously described (Dreyer et a. 1978). Only those muscle fibers with a resting potential of at least – 60 mV were used for these studies. The endplate was located under the microscope at 400 × magnification using Nomarski-interference optics. Two microelectrodes, filled with 3 M KCl and each with a resistance of 5 – 10 MΩ, were impaled into the muscle fiber on either side of the endplate. The muscle fiber was voltage clamped near the resting membrane potential (usually at – 80 mV). A micropipette filled with 2.5 M acetylcholine chloride (ACh) and with a resistance of 100 – 220 MΩ was placed 25 µm above the center of the endplate. Endplate currents generated by increasing doses of ionophoretically applied ACh were digitized, recorded and evaluated by a computer assisted measuring system (Nicolet Med 80). Dose-response curves were obtained by plotting peak endplate current (response) against an increasing charge passed through the ACh pipette (dose) on a double logarithmic scale. These curves were evaluated by using a co-operative model for the interaction between ACh molecules and the receptors, and a diffusion equation that was approximated using a theoretical model: diffusion from a point source (tip of the ACh pipette) to a circular area on the surface of the muscle fiber. For a given distance, z, of the ionophoretic pipette above the endplate, which can be determined micrometrically as well as from the time to peak of the endplate currents (Dreyer et al. 1978), the shape of the dose response curve depends on the geometry of the receptor distribution on the postsynaptic membrane. For evaluation of dose-response data, receptors were assumed to be homogeneously distributed over a circular area with its center at the center of the synapse and with a radius R large enough so that all receptors which contribute to the dose response curve were contained within this circle (see Hohlfeld et al. 1981). R was obtained from the best fit of the data by our model.

From the computer fit of the experimental dose-response curves estimations were made of the maximum ACh-induced conductance change per unit endplate surface (g_{max}), the apparent dissociation constant for the interaction between ACh molecules and the receptors (K), and the Hill-coefficient (n_H) as a measure of the co-operativity of the interaction (Dreyer et al. 1978).

ACh-induced noise was analyzed following the methods previously described (Dreyer et al. 1976b). ACh currents of 10 – 50 nA were applied for more than 30 s, and the resulting endplate currents were simultaneously recorded on a low gain DC-channel and on a high gain AC-channel (band pass between 3 and 1,000 Hz; active 6 pole Butterworth filter). Following analog-to-digital conversion, 20 records of 1,024 points were sampled at a rate of 2,000 Hz and stored. After analysis, background noise spectra were subtracted from the ACh induced noise spectra. From the computer fit of a Lorentzian curve to the resulting spectrum, the cut off frequency and the zero frequency amplitude were determined. Using these values, the mean life time of an open channel (τ) and the mean single channel conductance (γ) were calculated.

Results

Dose-response curves were obtained from 38 endplates of EDL and 20 endplates of soleus muscle fibers, isolated from 6 rats. Figure 1 shows typical ACh-dose response curves obtained under identical conditions from an endplate of an EDL and an endplate of a soleus muscle fiber isolated from the same rat. The striking difference between the curves is that the maximum current is substantially lower for the soleus endplate than for the EDL endplate, due to a reduced unit maximum conductance (g_{max}) in the soleus. In addition, the curve for the soleus endplate appears to be shifted to the right. However, analysis of the data shows that the dissociation constant of the soleus dose-response curve is not greater than that of EDL. This can be seen by normalization of the two curves with respect to the maximum peak currents. The steepness of the two curves in the low dose range is the same, suggesting that the Hill-coefficient (n_H) at the endplates of EDL and soleus muscle fibers is similar.

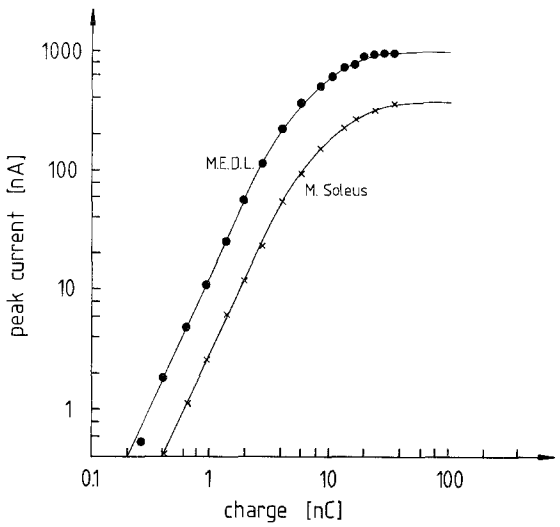

Fig. 1. Dose-response curves obtained from the endplates of a soleus muscle fiber and an EDL muscle fiber from the same rat. The responses were recorded under identical conditions. Temperature was 22° C, and the holding potential was – 70 mV. Dose-response parameters for the two curves are, for EDL (soleus): n_H: 2.2 (2.2), g_{max}: 22 nS/µm² (8.3 nS/µm²), K: 53 µM (48 µM)

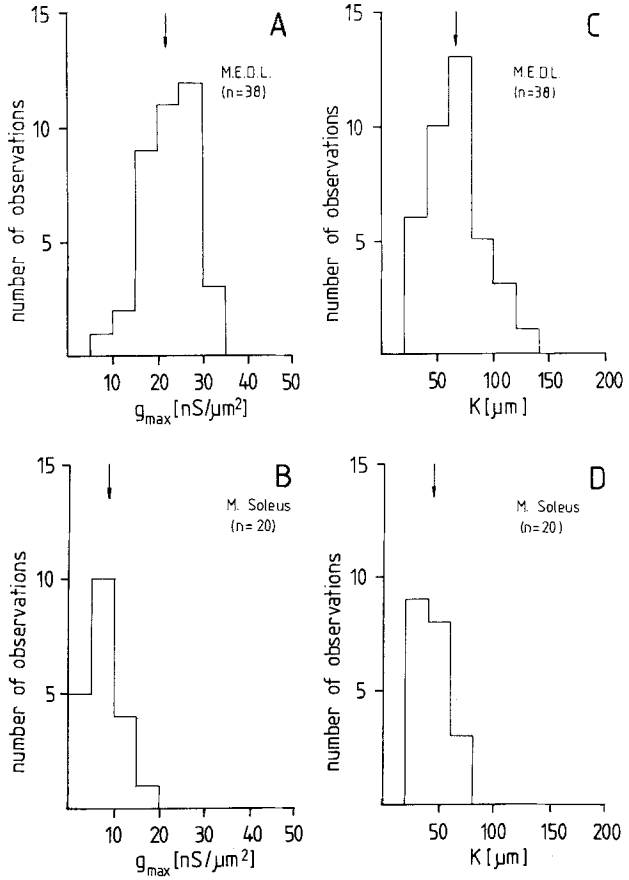

Fig. 2. Histograms of the distribution of g_{max} values in EDL (**A**) and soleus (**B**), as well as the K values in EDL (**C**) and soleus (**D**) endplates. The number of endplates is indicated in parentheses. *Arrows* indicate the respective arithmetic means. See Table 1

Table 1. Comparison of postjunctional properties of fast and slow muscle fibers in the rat. Temperature: 20–23°C. Values are Mean ± SEM (number of endplates)

Dose-response relations	EDL	Soleus
Maximum endplate conductance		
per unit surface area g_{max} (nS/µm²)	21.8 ± 0.9 (38)	8.2 ± 0.9 (20)***
Apparent dissociation constant K (µM)	65.9 ± 4.3 (38)	43.5 ± 3.3 (20)**
Hill-coefficient n_H	2.3 ± 0.1 (38)	2.2 ± 0.1 (20)
Single channel characteristics		
Mean conductance γ (pS)	24.6 ± 1.2 (14)	23.9 ± 1.2 (24)
Mean life time τ (ms)	0.80 ± 0.05 (14)	0.71 ± 0.03 (24)*
Average number of ionic channels		
per µm² of endplate surface	837 ± 35 (38)	343 ± 44 (20)***

Statistical significance of difference is given as * $P < 0.05$, ** $P < 0.01$, and *** $P < 0.001$

A summary of our data is given in Fig. 2 as well as in Table 1. Figure 2 A and B show histograms of the values for the maximum conductance per unit endplate area g_{max}, obtained from the ACh-dose response curves of all the endplates studied. The mean conductance (indicated by the arrow) in the soleus endplates was less than half that of the EDL endplates. In addition, in soleus some of the values are well below the minimum values found in EDL. Figure 2 C and D show similar histograms for the values of the apparent dissociation constant (K). In soleus the mean value for K was generally lower than in EDL.

Statistical analysis (t-test) of the dose response parameters is shown in Table 1. The mean g_{max} value in soleus was 62% lower ($P < 0.001$) than in EDL. Similarly, the mean K value in soleus was 34% smaller ($P < 0.01$) than in EDL. However, there was no significant difference between the values of the Hill-coefficient for the two kinds of endplates.

Dose response curves in EDL and soleus could best be fitted assuming that the radii R of the model endplate (see materials and methods section) range between 20–40 µm.

Using values for g_{max} and R from our response curves as well as γ obtained from noise analysis of ACh induced current fluctuations we calculated that on the average about $2.3 \times 10^6 \pm 0.11$ (38 fibers) channels in EDL and only $1.1 \times 10^6 \pm 0.08$ (20 fibers) in soleus can be opened at saturation.

Spectral density analysis of ACh-induced current fluctuations was carried out at 14 endplates of EDL and 24 endplates of soleus. Figure 3 A and B show typical ACh noise spectra obtained under identical conditions from the endplates of EDL and soleus muscle fibers isolated from the same rat. It is apparent that there are no major differences between the noise spectra of these two muscles and both spectra can be described by single Lorentzian curves. Analysis of such curves from all the enplates studied showed that there was no significant difference between EDL and soleus for the mean conductance of a single channel (γ), while the mean life time of the channel (τ) was slightly (11%) lower ($P < 0.01$) in soleus than in EDL endplates (Table 1).

Figure 4 shows some typical endplates in EDL (Fig. 4A) and soleus (Fig. 4B) after staining for ACh-esterase.

Stained areas are not homogeneously distributed over the entire endplate surface but rather show discontinuities. Similar patterns are found after labelling mammalian endplates with fluorescent α-bungarotoxin (Anderson and Cohen 1974; Peper et al. 1980). The shapes of both types of endplates (EDL and soleus) are essentially similar and do not differ appreciably from endplates in the omohyoid muscle (Dreyer et al. 1976a).

The overall shape of the endplates can be described mathematically as an ellipse with width a and length b. The length b, in 30 endplates each from 6 rats, ranged from 40–70 µm (35–50 µm) and a from 30–60 µm (20–40 µm) in EDL (soleus). The ratio of width to length was fairly constant in both types of muscles (mean ± S.E.M.): 0.59 ± 0.02 in EDL and 0.62 ± 0.05 in soleus. These findings concerning the overall dimensions of the endplates are comparable to those of other authors (Ellisman et al. 1976) and do not differ appreciably from preliminary observations made on endplates which were stained using immunofluorescence (Kaul et al. 1982). However, ACh-esterase stained areas and fluorescent areas do not seem to be congruent.

Interestingly, we found almost perfectly circular endplates in some EDL preparations (Fig. 4C). Similar endplates were not found in soleus. In some of the circular endplates the ACh-esterase staining was restricted to the circumference of the circle as in Fig. 4C, in others an irregular staining pattern over the entire surface was observed. This observation was not dependent on the time taken for the staining procedure.

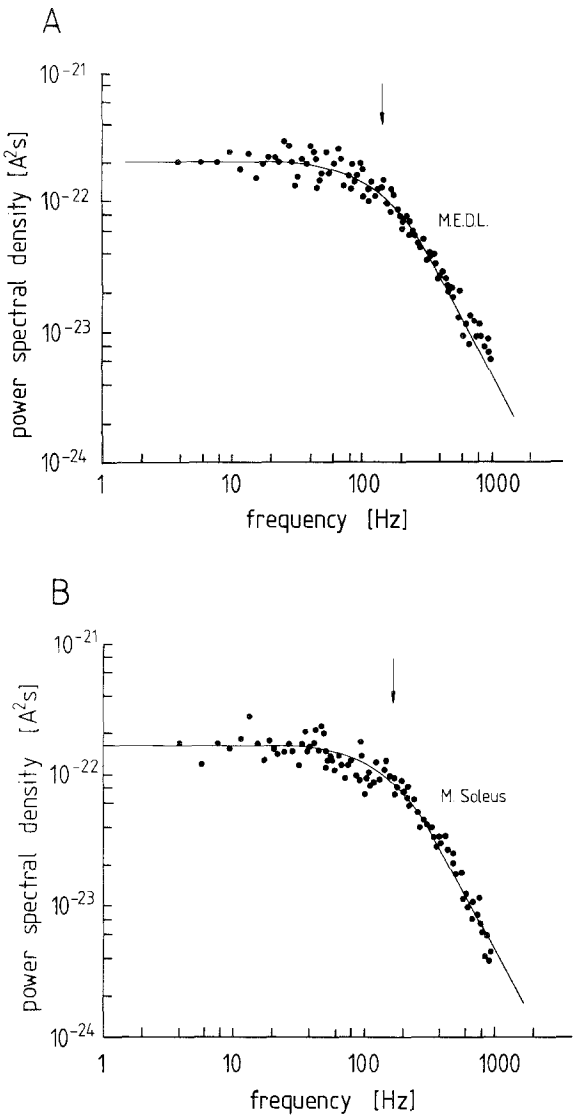

Fig. 3. Power density spectra calculated from ACh-induced endplate current noise, after subtracting the background noise spectra, at an EDL muscle fiber (**A**) and at a soleus muscle fiber (**B**) from the same rat, different from that used in Fig. 1. The current fluctuations were recorded under identical conditions at a temperature of 23°C, and a holding potential of −70 mV. The corresponding parameters of the spectra are, for EDL (soleus): cutoff frequency (*arrows*): 145 Hz (174 Hz), mean current: 30 nA (32 nA), τ: 1.10 ms (0.92 ms), and γ: 23.3 pS (22.1 pS)

Discussion

The present investigation shows that, despite many similarities, characteristic differences exist between the electrophysiological properties of endplates in the EDL and soleus muscles of the rat. Analysis of dose response curves shows that there is no significant difference in the Hill coefficient suggesting that the cooperative interaction between subunits of ACh receptors are similar at the endplates of both EDL and soleus muscle fibers. However, the apparent dissociation constant, K, is 34% smaller in soleus than in EDL. As K pertains to both the ACh binding step and to the conformational change of the ACh receptor, a smaller K could mean either a higher affinity of ACh receptors for ACh, or a more rapid change from the closed to the open channel configuration, or both. The method used in this paper cannot discriminate between these possibilities.

The most striking difference between the two types of muscle concerned the maximum conductance per unit surface area of endplate, g_{max}, which is about 60% lower in soleus than in EDL. A lower g_{max} could be due to a lower single channel conductance γ, or to a smaller number of functioning ACh receptors at the endplate membrane. Although the single channel life-time τ was slightly (11%) lower in soleus, γ was found to be similar in EDL and soleus muscles. Hence the lower g_{max} could be due to the presence of a smaller number of functioning ACh receptors per unit area of the endplate in soleus than in EDL.

Since we know γ, we can convert g_{max} into the number of ionic channels opened per unit surface area of the endplate at saturating agonist concentrations. Thus, with a g_{max} of 20.6 nS/μm^2 and γ of 24.6 pS, an average of about 840 ionic channels can be opened per μm^2 of EDL endplates. Similarly, with a g_{max} of 8.8 nS/μm^2 and γ of 23.9 pS, an average of only 340 channels can be opened per μm^2 of soleus endplates.

An estimate of the total number of open ionic channels at saturation can be obtained, using the values of the radius R for our model circular endplate derived from computer fits to actual dose-response data. Thus, an average of about 2×10^6 channels can be opened by ACh in EDL endplates, but only 1×10^6 channels in soleus endplates. The values for these electrophysiological parameters of the EDL endplates are similar to those of the endplates of the rat omohyoideus muscle, which is also a fast muscle (Hohlfeld et al. 1981). However, the values for K and g_{max} for the soleus endplate are significantly less than those found for the omohyoideus endplate.

It should be pointed out that the density of ionic channels determined by us assumes a homogeneous distribution of these channels over the entire postsynaptic membrane. The actual distribution of receptors, however, is highly inhomogeneous as cen be seen from morphological studies of mammalian endplates using various techniques (Fambrough 1979, review and further literature).

Thus the density of α-bungarotoxin binding sites is highest at the crest of the junctional folds of the endplate, while at the bottom of the folds it is only a tenth of the density at the crest (Fertuck and Salpeter 1974; Albuquerque et al. 1974).

The inhomogeneity of receptor distribution over the whole mammalian endplate can be impressively demonstrated by fluorescent α-bungarotoxin staining of ACh receptors (Anderson and Cohen 1974; Peper et al. 1980).

It was shown in a detailed morphological study on EDL and soleus endplates that despite gross morphological differences, packing densities of putative ACh receptors in freeze-fracture electron micrographs are similar for the two types of muscle (Ellismann et al. 1976). At the tops of junctional folds macromolecular specializations had densities of 1,800–2,300/μm^2 in both EDL and soleus. However, no information was provided by these authors about the distribution and total amount of putative receptors over the whole endplate.

A comparative estimate has been made of the number of radioactively labelled α-bungarotoxin binding sites for EDL and soleus of mouse which indicates that more than 34% more binding sites per endplate exist in soleus than in EDL (Robbins et al. 1980). These authors subtracted the values obtained from equal lengths of endplate free regions from those containing endplates in order to calculate the number of junctional binding sites. Despite these precautions it cannot

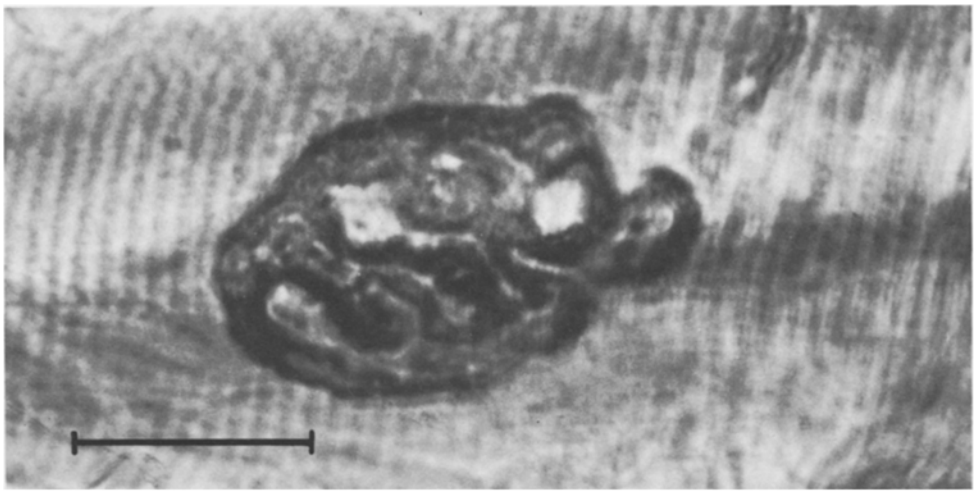

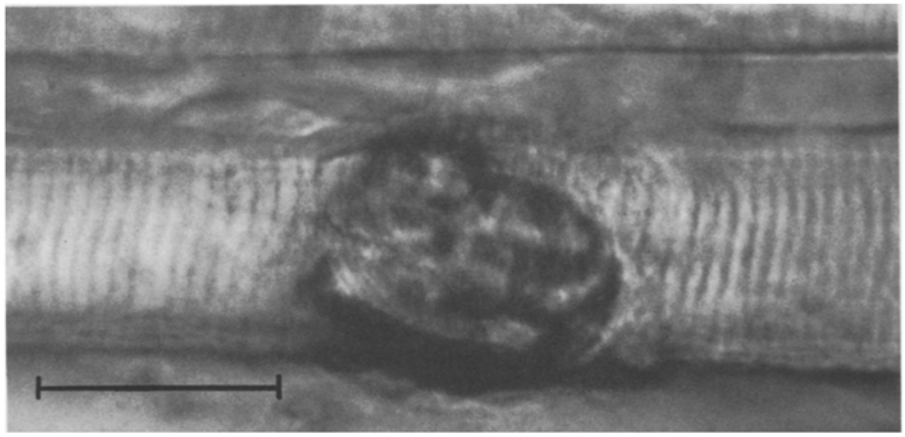

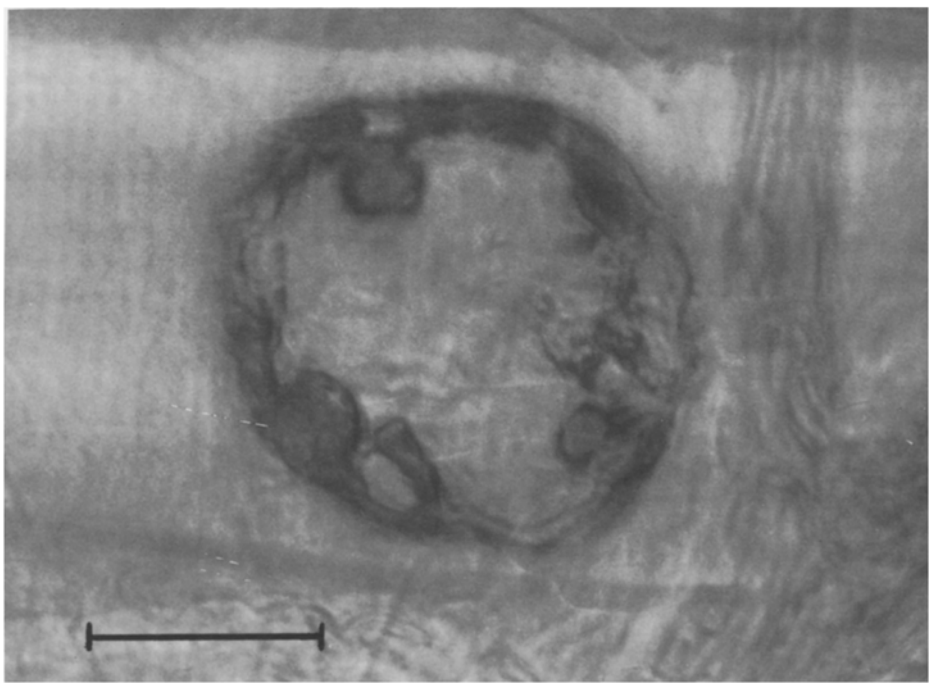

Fig. 4
Typical endplates stained for ACh esterase in rat EDL muscle fiber (**A**, *top*) and soleus muscle fiber (**B**, *middle*). In some EDL muscle fibers the endplate appeared as a perfect circle (**C**, *below*). Such a shape was never seen in soleus muscle fibers. The calibration bar represents 20 μm. The photographs were taken using a microscope fitted with Nomarski interference optics and a water immersion objective (40 ×)

be excluded that perijunctional receptors may have substantially contributed to their estimates.

Soleus muscle fibers show a considerably greater extrajunctional ACh sensitivity than EDL muscle fibers. This extrajunctional sensitivity is graded being highest in the immediate vicinity of the endplate and lowest in the endplate free region (Miledi and Zelena 1966; Albuquerque et al. 1974). Even though we did not quantify this finding, we also observed considerable ACh sensitivity in the vicinity of the endplates in soleus but not in EDL. This sensitivity to ACh in the vicinity of the soleus endplate could be due to perijunctional receptors similar to those which often occur at frog endplates (Dreyer et al. 1976b). Thus the method used by Robbins et al. (1980) could result in a considerable overestimation in the determination of bungarotoxin binding sites on soleus endplates.

Comparing our results obtained by quantitative ionophoresis with those of morphological studies it should be borne in mind that, at present, no exact values have been determined relating α-bungarotoxin sites and macromolecular structures (putative ACh receptors) in freeze fracture studies to ACh controlled ionic channels in the living mammalian endplate.

The factors relating the total population of receptors in the closed conformation to the open ionic channels are quite complex. These factors are, among others, dependent on the so-called "efficacy" of the drug used to open the channels and on the phenomenon of desensitization (Peper et al. 1982, review and further literature). For the safety of transmission from nerve to muscle the number of "functional receptors" (ionic channels) in the postsynaptic membrane is most important.

Our ionophoretic method provides evidence that the average density of the ionic channels at the endplate, and thus the density of functional ACh receptors is significantly lower in the slow muscle, soleus, than in the fast muscle, EDL, even though some areas with a similar channel density could exist in both muscles. This lower overall density of ACh receptors in the slow muscle could provide an explanation for the earlier observations showing blockade of neuromuscular transmission in the cat soleus muscle on exposure to much lower concentrations of *d*-tubocurarine than was needed to cause the block in the fast muscle, anterior tibialis (Paton and Zaimis 1951). Owing to the lower density of the ACh receptors, the slow muscle could have a lower margin of safety for neuromuscular transmission than the fast muscle. In agreement with this, we found in preliminary studies that the soleus is more sensitive to experimental autoimmune myasthenia gravis than the EDL (Pagala et al. 1983, in preparation). Interestingly some preliminary results on electrophysiological investigations show a similarly low value for g_{max} at some endplates of the rat diaphragm.

It must be pointed out, however, that even though the average density of the functional ACh receptors is lower at the soleus endplate than at the EDL endplate, it may still be far in excess of that needed for normal neuromuscular transmission.

References

Albuquerque EX, McIsaac RJ (1970) Fast and slow mammalian muscles after denervation. Exp Neurol 26:183–202

Albuquerque EX, Thesleff S (1968) A comparative study of membrane properties of innervated and chronically fast and slow skeletal muscles of the rat. Acta Physiol Scand 73:471–480

Albuquerque EX, Barnard EA, Porter CW, Warnick JE (1974) The density of acetylcholine receptors and their sensitivity in the postsynaptic membrane of muscle endplates. Proc Natl Acad Sci USA 71:2818–2822

Anderson CR, Stevens CF (1973) Voltage clamp analysis of acetylcholine produced endplate current fluctuations at frog neuromuscular junction. J Physiol 235:655–691

Anderson MJ, Cohen MW (1974) Fluorescent staining of acetylcholine receptors in vertebrate skeletal muscle. J Physiol 237:385–400

Ariano MA, Armstrong RB, Edgerton VR (1973) Hindlimb muscle fiber populations of five mammals. J Histochem Cytochem 21:51–55

Barany M, Barany K, Rickard T, Volpe A (1965) Myosin of fast and slow muscles of the rabbit. Arch Biochem Biophys 109:185–191

Barnard EA, Rymaszewska T, Wieckowski J (1971) Cholinesterase at individual neuromuscular junctions. In: Triggle DJ, Moran JF, Barnard EA (eds) Cholinergic ligand interactions. Academic Press, New York, pp 175–200

Close R (1964) Dynamic properties of fast and slow skeletal muscles of the rat during development. J Physiol 173:74–95

Dreyer F, Mueller KD, Peper K, Sterz R (1976a) The M. omohyoideus of the mouse as a convenient mammalian muscle preparation: a study of junctional and extrajunctional acetylcholine receptors by noise analysis and cooperativity. Pflügers Arch 367:115–122

Dreyer F, Walther Chr, Peper K (1976b) Junctional and extrajunctional receptors in normal and denervated frog muscle fibers. Pflügers Arch 366:1–9

Dreyer F, Peper K, Sterz R (1978) Determination of dose-response curves by quantitative ionophoresis at the frog neuromuscular junction. J Physiol 281:395–419

Eccles LC, Eccles RM, Lundberg A (1958) The action potentials of the alpha motoneurons supplying fast and slow muscles. J Physiol 142:275–291

Ellisman MH, Rash JE, Staehlin LA, Porter KR (1976) Studies of excitable membranes. II. A comparison of specializations at neuromuscular junctions and non-junctional sarcolemmas of mammalian fast and slow twitch muscle fibers. J Cell Biol 68:752–774

Fambrough DM (1979) Control of acetylcholine receptors in skeletal muscle. Physiol Rev 59:165–227

Fertuck HC, Salpeter MM (1974) Localization of acetylcholine receptor by ^{125}I-labelled bungarotoxin at mouse endplates. Proc Natl Acad Sci USA 71:1376–1378

Goldspink DF, Harris JB, Park DC, Parsons NE, Pennington RJ (1971) Quantitative enzyme studies in deneravated extensor digitorum longus and soleus of rats. J Biochem 2:427–433

Guth L, Samaha FJ (1969) Qualitative differences between actomyosin ATPase of slow and fast mammalian muscle. Exp Neurol 25:138–152

Hohlfeld R, Sterz R, Kalies I, Peper K, Wekerle H (1981) Neuromuscular transmission in experimental autoimmune myasthenia gravis (EAMG). Pflügers Arch 390:156–160

Karnovsky MJ, Roots L (1964) A direct coloring thiocholine method for cholinesterase. J Histochem Cytochem 12:219–221

Kaul M, Hammer H, Sterz R, Peper K (1982) Immunofluorescence of the acetylcholine receptor in endplates. Pflügers Arch 394 (Suppl): R51

McArdle JJ, Albuquerque EX (1973) A study of the reinnervation of fast and slow mammalian muscles. J Gen Physiol 61:1–23

Miledi R, Zelena J (1966) Sensitivity to acetylcholine in rat slow muscles. Nature 210:855–856

Nachmias VT, Padykula HA (1958) A histochemical study of normal and denervated and white muscle of the rat. J Biophys Biochem Cytol 4:47–57

Paton WDM, Zaimis EJ (1951) The action of *d*-tubocurarine and of decamethonium on respiratory and other muscles in the cat. J Physiol 112:311–331

Peper K, Sterz R, Bradley RJ (1980) Effects of drugs and antibodies on the postsynaptic membrane of the neuromuscular junction. Ann NY Acad Sci 377:519–543

Peper K, Bradley RJ, Dreyer F (1982) The acetylcholine receptor at the neuromuscular junction. Physiol Rev 62:1271–1340

Robbins N, Olek A, Kelly SS, Takach P, Christopher M (1980) Quantitative study of motor endplates in muscle fibers dissociated by a simple procedure. Proc R Soc Lond B 209:555–562

Stein JM, Padykula HA (1962) Histochemical classification of individual skeletal muscle fibers of the rat. Am J Anat 110:103–115

Sterz R, Pagala MKD, Peper K (1982) Post-junctional properties of motor endplates in mammalian fast and slow muscles. Fed Proc 41:8680

Tonge DA (1974) Chronic effects of botulinum toxin on neuromuscular transmission and sensitivity to acetylcholine in slow and fast skeletal muscle of the mouse. J Physiol 241:127–139

Yonemura K (1967) Resting and action potentials in red and white muscle of the rat. Jpn J Physiol 17:708

Received December 6, 1982/Accepted February 26, 1983